

See discussions, stats, and author profiles for this publication at:  
<https://www.researchgate.net/publication/11502766>

# Conformational diversity of T-kinin in DMSO, water and HFA

ARTICLE *in* EUROPEAN JOURNAL OF MEDICINAL CHEMISTRY · MARCH 2002

Impact Factor: 3.45 · DOI: 10.1016/S0223-5234(01)01323-X · Source: PubMed

---

CITATIONS

5

---

READS

21

3 AUTHORS, INCLUDING:



Prashant V Desai

Eli Lilly

49 PUBLICATIONS 1,493 CITATIONS

SEE PROFILE



Sudha Srivastava

Tata Institute of Fundamental Research

95 PUBLICATIONS 822 CITATIONS

SEE PROFILE

## Original article

## Conformational diversity of T-kinin in DMSO, water and HFA

Prashant Desai <sup>a</sup>, Evans Coutinho <sup>a,\*</sup>, Sudha Srivastava <sup>b</sup><sup>a</sup> Department of Pharmaceutical Chemistry, Bombay College of Pharmacy, Kalina, Mumbai 400 098, India<sup>b</sup> Tata Institute of Fundamental Research, National Facility for High Field NMR, Homi Bhabha Road, Navy Nagar, Mumbai 400 005, India

Received 31 July 2001; received in revised form 28 November 2001; accepted 29 November 2001

## Abstract

T-kinin (Ile-Ser-BK) is related to BK in its biological profile, but unlike BK, is more resistant to the action of ACE. A detailed NMR and molecular modeling study of T-kinin has been carried out in three diverse media: water (pH 4.0), DMSO-*d*<sub>6</sub> and HFA solution. In DMSO-*d*<sub>6</sub>, T-kinin adopts a structure with two tandem  $\beta$ -turns: the first at the mid segment tetrad Pro<sup>4</sup>-Pro<sup>5</sup>-Gly<sup>6</sup>-Phe<sup>7</sup> (type I) and the C-terminal end Ser<sup>8</sup>-Pro<sup>9</sup>-Phe<sup>10</sup>-Arg<sup>11</sup> harbors the second turn (also type I). While the first  $\beta$ -turn is lost in presence of water, the second persists. In HFA, NMR reveals a  $\alpha$ -helix like structure spanning residues Arg<sup>3</sup> to Arg<sup>11</sup>. Structures with *cis* peptide bonds (XX-Pro) have been observed for T-kinin in DMSO-*d*<sub>6</sub> but not in water and HFA. Differences in the structures of BK and T-kinin in water may explain their susceptibility/resistance to the action of ACE. © 2002 Éditions scientifiques et médicales Elsevier SAS. All rights reserved.

**Keywords:** T-kinin; Conformation;  $\beta$ -Turn; NMR; MD simulations

## 1. Introduction

Kinins are potent vasodilator oligopeptides that contain the nonapeptide bradykinin (BK, Arg<sup>1</sup>-Pro-Pro-Gly-Phe<sup>5</sup>-Ser-Pro-Phe-Arg<sup>9</sup>) as part of their sequence. Kinins have a variety of physiological effects such as regulation of blood pressure, renal and cardiac function, and have been implicated in pathogenesis of hypertension and inflammation. Kinins act via two types of receptors, type 1 (B1) and type 2 (B2), with B2

receptors predominating [1]. Potent vasodilatory and algesic activities of the typical kinin BK, are well documented [2–4]. Kinins are mainly inactivated by angiotensin converting enzyme (ACE). C-terminal cleavage by ACE, results in an inactive metabolite, BK (1–7) [5].

One of several peptides related to bradykinin is T-kinin (Ile-Ser-BK), first isolated from rat plasma [6]. T-kinin exhibits a variety of activities, like regulation of blood vessels, airway extravasation and uterine contraction, through stimulation of B2 receptors, in species like rat, dog, hamster and cat [7–12]. Moreover, it is also reported to be involved in inflammation [13] and causes release of prostaglandins [8]. T-kinin is produced in considerable amounts by human tissues under certain conditions like ovarian carcinoma [14,15]. Although, in some models (dog carotid and renal arteries), T-kinin is found to be less potent as compared to BK [16], in few others (cat hind limb vascular bed and rat uterus) it exhibits a potency equivalent to BK [8,11]. It is interesting to note that T-kinin is resistant to C-terminal cleavage by ACE, whereas BK, is rapidly inactivated by ACE [17].

**Abbreviations:** BK, bradykinin; ACE, angiotensin converting enzyme; TFE, trifluoroethanol; SDS, sodium dodecyl sulfate; DDS, sodium 2,2-dimethyl-2-silapentane-5-sulfonate; HFA, hexafluoroacetone; HSQC, hetero nuclear single quantum coherence; TOCSY, total correlated spectroscopy; ROESY, rotating frame nuclear Overhauser effect spectroscopy; DQF-COSY, double quantum filtered correlated spectroscopy; NOESY, nuclear Overhauser effect spectroscopy; CSI, chemical shift index; MD, molecular dynamics; IRMA, iterative relaxation matrix analysis; RMSD, root mean squared deviation; Hyp, trans-4-hydroxy-L-proline; Thi,  $\beta$ -(2-thienyl)-L-alanine; Cpg,  $\alpha$ -cyclo-pentyl-glycine.

\* Correspondence and reprints.

E-mail address: [evans@im.eth.net](mailto:evans@im.eth.net) (E. Coutinho).

Several studies have reported the structure of BK in different environments like water [18], DMSO- $d_6$  [19,20], aq. TFE [21], and SDS micelles [22]. While a flexible random coil like conformation was proposed for BK in water [18], in micelles [22] it was found to possess a  $\beta$ -turn at the C-terminal end spanning residues Ser<sup>6</sup>-Pro<sup>7</sup>-Pro<sup>8</sup>-Arg<sup>9</sup>. We had proposed a two  $\beta$ -turn conformation covering residues Pro<sup>2</sup>-Pro<sup>3</sup>-Gly<sup>4</sup>-Phe<sup>5</sup> and Ser<sup>6</sup>-Pro<sup>7</sup>-Pro<sup>8</sup>-Arg<sup>9</sup> for BK in DMSO- $d_6$  [19]. BK has been reported to exist in a mixture of at least two different conformers in aq. TFE [21]; one being an all *trans* extended structure, and the other, a structure with a *cis* Pro<sup>2</sup>-Pro<sup>3</sup> bond in a type VI  $\beta$ -turn between residues Arg<sup>1</sup>-Gly<sup>4</sup>.

Modifications to BK have been made to understand the structural requirements for biological activity. Alteration of amino acids at both the N- and C-termini has a profound effect on activity. Thus, des[Arg<sup>1</sup>]-BK and des[Arg<sup>9</sup>]-BK are devoid of activity [23]. Replacement of Arg<sup>1</sup> by Lys retains only 10% of the activity [24] and the peptide was shown to have only a single C-terminal  $\beta$ -turn [25]. A replacement of Phe<sup>8</sup> by Tyr significantly reduces the potency [26]. This was explained to arise from a total loss of  $\beta$ -turn structure [27]. Addition of Tyr at the N-terminal retains 90% of the activity of native BK [28]. This is due to the fact that its conformation was found to be similar to BK (a two tandem  $\beta$ -turn structure) [29]. The 10% loss in activity was attributed to *cis* peptide bonds, which are absent in the two  $\beta$ -turn structure of BK.

There is thus, a strong correlation between the conformations of BK analogs vis a vis' the conformation of native BK and biological activity. Continuing with our studies on kinins, we have undertaken an investigation of the conformation of T-kinin, to understand its higher stability to ACE, compared to native BK. The conformation has been investigated in water (pH 4.0), DMSO- $d_6$  and 40% HFA solution.

It is now well established that solvents like TFE and HFA are invaluable media for probing biomolecular structure, function, dynamics and protein folding. There is strong evidence that structures seen in such solvents could be similar to those adopted by the peptide in their active conformation (generally the bound form). The study of the conformation and dynamics of membrane bound peptides is a challenging one. A number of model systems have been suggested to mimic features of the membrane. It is now emerging that TFE and HFA are suitable model systems for the membrane [30,31].

## 2. Results and discussion

The <sup>1</sup>H chemical shifts of T-kinin along with temperature coefficients of amide protons, and <sup>3</sup>J<sub>NH $\alpha$</sub>  coupling constants, in the three solvents viz. water, DMSO- $d_6$  and HFA are presented in Tables 1–3, respectively. The <sup>13</sup>C chemical shifts in DMSO- $d_6$  and HFA, as obtained from HSQC spectra, are listed in Table 4. The HSQC spectrum of water was of 'poor quality', consequently the <sup>13</sup>C chemical shifts are not reported in Table 4. As an example, a portion of the TOCSY spectrum of the peptide in DMSO- $d_6$ , showing the spin systems, and a NOESY spectrum outlining the sequential assignments, are presented in Figs. 1 and 2a, respectively. Average values of torsion angles of structures obtained by the three MD simulations, are given in Tables 5–7, respectively. Analysis of the ensemble of structures obtained from MD simulations, is given in Table 8.

### 2.1. Conformation in water

The NOESY spectrum in water displayed very few inter-residue cross peaks, mainly the  $\alpha$ ,N (*i*, *i* + 1) sequential peaks (Fig. 3). Only one set of peaks was

Table 1  
Chemical shifts ( $\delta$  ppm), <sup>3</sup>J<sub>NH $\alpha$</sub>  (Hz) and temperature coefficients of NH chemical shifts (ppb K<sup>-1</sup>) of T-Kinin in water <sup>a,b</sup>

Residue	NH	$\alpha$ H	$\beta$ H	Others	<sup>3</sup> J <sub>NH<math>\alpha</math></sub>	Temperature coefficient
Ile <sup>1</sup>	–	3.91	1.97	$\gamma$ CH <sub>2</sub> 1.49, 1.22; $\gamma$ CH <sub>3</sub> 0.99, $\delta$ CH <sub>3</sub> 0.92	–	–
Ser <sup>2</sup>	8.67	4.54	3.86, 3.79	–	5.9	4.0
Arg <sup>3</sup>	8.44	4.60	1.72, 1.68	$\gamma$ CH <sub>2</sub> 1.58, $\delta$ CH <sub>2</sub> 3.06, 2.97, $\epsilon$ NH 7.13	–	5.0
Pro <sup>4</sup>	–	4.70	2.37, 1.89	$\gamma$ CH <sub>2</sub> 2.01, $\delta$ CH <sub>2</sub> 3.78, 3.48	–	–
Pro <sup>5</sup>	–	4.40	2.28, 1.89	$\gamma$ CH <sub>2</sub> 2.05, $\delta$ CH <sub>2</sub> 3.82, 3.66	–	–
Gly <sup>6</sup>	8.43	3.93, 3.85	–	–	–	4.8
Phe <sup>7</sup>	7.99	4.55	3.08, 3.02	Ar. 7.12–7.31	8.0	3.9
Ser <sup>8</sup>	8.09	4.66	3.73	–	5.9	3.8
Pro <sup>9</sup>	–	4.29	2.16, 1.68	$\gamma$ CH <sub>2</sub> 1.89, $\delta$ CH <sub>2</sub> 3.57	–	–
Phe <sup>10</sup>	7.99	4.62	3.19, 2.95	Ar. 7.25–7.37	5.9	3.1
Arg <sup>11</sup>	7.73	4.14	1.81, 1.68	$\gamma$ CH <sub>2</sub> 1.54, $\delta$ CH <sub>2</sub> 3.16, $\epsilon$ NH 7.16	7.8	2.4

<sup>a</sup> Chemical shifts were obtained at 298 K.

<sup>b</sup> Pairs of geminal protons *x* (*x* =  $\alpha$ ,  $\beta$ ,  $\gamma$ ,  $\delta$ ) are not assigned stereospecifically. When two distinct lines were observed, the larger chemical shift was arbitrarily assigned to *x* and the smaller to *x'*.

Table 2

Chemical shifts ( $\delta$  ppm),  $^3J_{\text{NH}\alpha}$  (Hz) and temperature coefficients of NH chemical shifts (ppb K $^{-1}$ ) of T-kinin in DMSO- $d_6$  <sup>a</sup>

Residue	NH	$\alpha$ H	$\beta$ H	Others	$^3J_{\text{NH}\alpha}$	Temperature coefficient
Ile <sup>1</sup>	9.15	3.06	1.68	$\gamma$ CH <sub>2</sub> 1.35, 1.07; $\gamma$ CH <sub>3</sub> 0.85, $\delta$ CH <sub>3</sub> 0.81	–	6.3
Ser <sup>2</sup>	8.09	4.32	3.61, 3.48	–	–	1.2
Arg <sup>3</sup>	8.02	4.49	1.64, 1.50	$\gamma$ CH <sub>2</sub> 1.54, $\delta$ CH <sub>2</sub> 3.02	7.4	2.5
Pro <sup>4</sup>	–	4.58	2.19, 1.79	$\gamma$ CH <sub>2</sub> 1.79, $\delta$ CH <sub>2</sub> 3.66, 3.29	–	–
Pro <sup>5</sup>	–	4.27	2.03, 1.77	$\gamma$ CH <sub>2</sub> 1.95, $\delta$ CH <sub>2</sub> 3.67, 3.51	–	–
Gly <sup>6</sup>	8.57	3.87, 3.43	–	–	–	0.4
Phe <sup>7</sup>	8.18	4.51	2.99, 2.82	Ar. 7.17–7.27	7.6	0.7
Ser <sup>8</sup>	8.33	4.55	3.74	–	5.7	2.9
Pro <sup>9</sup>	–	4.29	1.87, 1.41	$\gamma$ CH <sub>2</sub> 1.64, 1.26, $\delta$ CH <sub>2</sub> 3.57	–	–
Phe <sup>10</sup>	7.86	4.42	3.19, 2.68	Ar. 7.22–7.49	8.6	2.5
Arg <sup>11</sup>	7.29	3.91	1.75, 1.63	$\gamma$ CH <sub>2</sub> 1.47, 1.44, $\delta$ CH <sub>2</sub> 3.05 $\epsilon$ NH 6.94	–	1.0

<sup>a</sup> See footnotes under Table 1.

Table 3

Chemical shifts ( $\delta$  ppm),  $^3J_{\text{NH}\alpha}$  (Hz) and temperature coefficients of NH chemical shifts (ppb K $^{-1}$ ) of T-kinin in HFA <sup>a,b</sup>

Residue	NH	$\alpha$ H	$\beta$ H	Others	$^3J_{\text{NH}\alpha}$	Temperature coefficient
Ile <sup>1</sup>	–	3.95	1.99	$\gamma$ CH <sub>2</sub> 1.52, 1.22; $\gamma$ CH <sub>3</sub> 1.00, $\delta$ CH <sub>3</sub> 0.90	–	–
Ser <sup>2</sup>	8.48	4.64	3.94	–	6.8	2.9
Arg <sup>3</sup>	8.17	4.63	1.68	$\gamma$ CH <sub>2</sub> 1.51, $\delta$ CH <sub>2</sub> 2.99, 2.79, $\epsilon$ NH 6.94	6.8	3.1
Pro <sup>4</sup>	–	4.66	2.37	$\gamma$ CH <sub>2</sub> 2.02, $\delta$ CH <sub>2</sub> 3.76, 3.41	–	–
Pro <sup>5</sup>	–	4.42	2.30, 1.93	$\gamma$ CH <sub>2</sub> 2.08, $\delta$ CH <sub>2</sub> 3.84, 3.65	–	–
Gly <sup>6</sup>	8.25	4.04, 3.84	–	–	–	5.2
Phe <sup>7</sup>	7.81	4.44	3.15, 2.99	Ar. 7.19–7.32	5.1	2.1
Ser <sup>8</sup>	7.53	4.65	3.85, 3.66	–	6.8	0.2
Pro <sup>9</sup>	–	4.29	2.09, 1.61	$\gamma$ CH <sub>2</sub> 1.81, 1.43, $\delta$ CH <sub>2</sub> 3.54, 3.41	–	–
Phe <sup>10</sup>	7.49	4.65	3.26, 2.86	Ar. 7.24–7.38	6.8	1.6
Arg <sup>11</sup>	7.83	4.40	1.94, 1.78	$\gamma$ CH <sub>2</sub> 1.63, $\delta$ CH <sub>2</sub> 3.19, $\epsilon$ NH 7.08	7.8	1.3

<sup>a</sup> Chemical shifts were obtained at 283 K.<sup>b</sup> See footnote under Table 1.

observed, indicating the presence of a single predominant conformation for the peptide in water. Cross peaks between Arg<sup>3</sup>  $\alpha$ H-Pro<sup>4</sup>  $\delta$ H, Pro<sup>4</sup>  $\alpha$ H-Pro<sup>5</sup>  $\delta$ H and Ser<sup>8</sup>  $\alpha$ H-Pro<sup>9</sup>  $\delta$ H, suggest a *trans* conformation for all proline residues. It may be noted that, native BK was also found in a *trans* arrangement of proline residues in water [32].

Among all residues, only Arg<sup>11</sup> amide proton has a relatively low temperature coefficient. Lack of NMR data diagnostic of secondary structure, made it difficult to pinpoint the structural motif contributing to the low temperature coefficient for Arg<sup>11</sup>. We have taken recourse to ‘free’ MD simulations to determine the structural pattern around the C-terminal end. Nearly 40% of the simulated structures in the ‘free’ MD simulations are characterized by a  $\beta$ -turn around the segment Ser<sup>8</sup>-Pro<sup>9</sup>-Phe<sup>10</sup>-Arg<sup>11</sup>. The presence of a  $\beta$ -turn at the C-terminal end is also echoed by the theoretical methods. The Chou and Fasman calculations read a high probability for a  $\beta$ -turn for the sequence Ser-Pro-Phe-Arg [18]. Also, the Garnier–Osguthorpe–Robson secondary structure prediction method indicates the probability of a turn like structure at the C-terminal.

Lack of significant nOe’s and relatively high amide temperature coefficients for residues at ‘N-terminal’, indicate an extended or random coil like structure for this portion of the peptide.

The MD simulations with restraints returned a type I  $\beta$ -turn for these residues (Fig. 4a), with an average pair-wise RMSD of 1.51 (Table 8). A constraint free minimization of these 25 MD structures retained the  $\beta$ -turn at the C-terminal in all structures.

These results indicate that T-kinin has a different conformation from BK, in water. The latter is known to exist in several conformational states in water, all of which are nearly extended in form, or are best described as a random coil [18]. The conformational differences between T-kinin and BK at their C-terminal ends, may relate to their susceptibility to ACE. As mentioned earlier, ACE reduces BK to a heptapeptide by cleaving two amino acids from its C-terminal. This is made possible by the nearly extended state of the C-terminal end. Thus, folding of the C-terminal in a  $\beta$ -turn in T-kinin, may cause it to bind in a manner that resists hydrolysis by ACE, or may cause it to bind very weakly to ACE, thus escaping its proteolytic action.

## 2.2. Conformation in DMSO- $d_6$

A significant number of inter-residue nOe's observed in DMSO- $d_6$  may at least partly arise from a rigid conformation of T-kinin in this solvent compared to water. A weak cross peak between Ser<sup>8</sup>  $\alpha$ H-Pro<sup>9</sup>  $\alpha$ H (Fig. 2b) suggests the presence of a minor component

Table 4  
<sup>13</sup>C chemical shifts ( $\delta$  ppm) of T-kinin in DMSO- $d_6$  and HFA <sup>a</sup>

Solvent	Residue	$\alpha$ C	$\beta$ C	$\gamma$ C	$\delta$ C
DMSO	Ile <sup>1</sup>	62.7	41.5	27.1, 19.3	15.2
HFA		61.5	39.9	27.4, 17.1	13.6
DMSO	Ser <sup>2</sup>	57.9	65.4	—	—
HFA		58.4	64.6	—	—
DMSO	Arg <sup>3</sup>	53.5	31.7	27.8	43.8
HFA		54.2	31.6	27.3	43.8
DMSO	Pro <sup>4</sup>	61.2	30.9	28.0	50.2
HFA		62.3	31.2	27.8	51.1
DMSO	Pro <sup>5</sup>	63.1	32.5	28.2	50.3
HFA		64.3	32.3	27.9	51.0
DMSO	Gly <sup>6</sup>	45.4	—	—	—
HFA		46.0	—	—	—
DMSO	Phe <sup>7</sup>	57.5	40.9	—	—
HFA		59.1	40.6	—	—
DMSO	Ser <sup>8</sup>	56.1	65.4	—	—
HFA		55.7	64.8	—	—
DMSO	Pro <sup>9</sup>	63.2	32.2	27.2	50.3
HFA		64.0	32.2	27.0	51.2
DMSO	Phe <sup>10</sup>	57.8	41.0	—	—
HFA		58.4	40.0	—	—
DMSO	Arg <sup>11</sup>	57.3	32.8	28.2	44.1
HFA		55.6	31.4	27.5	43.8

<sup>a</sup> Chemical shifts were obtained at 298 K in DMSO and at 283 K in HFA.

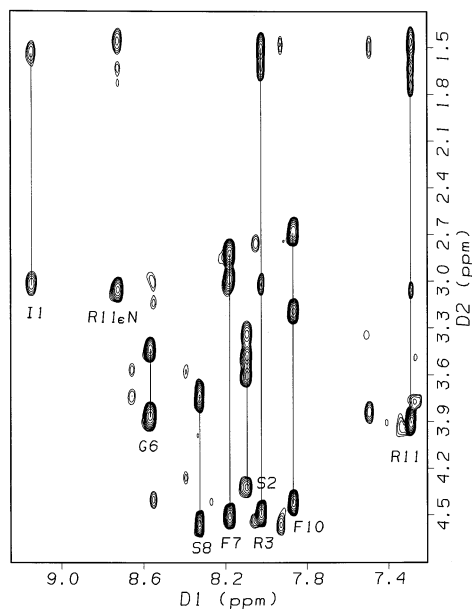


Fig. 1. TOCSY spectrum (500 MHz) of T-kinin in DMSO- $d_6$  at 298 K; D1: 7.20–9.25 ppm, D2: 1.25–4.80 ppm.

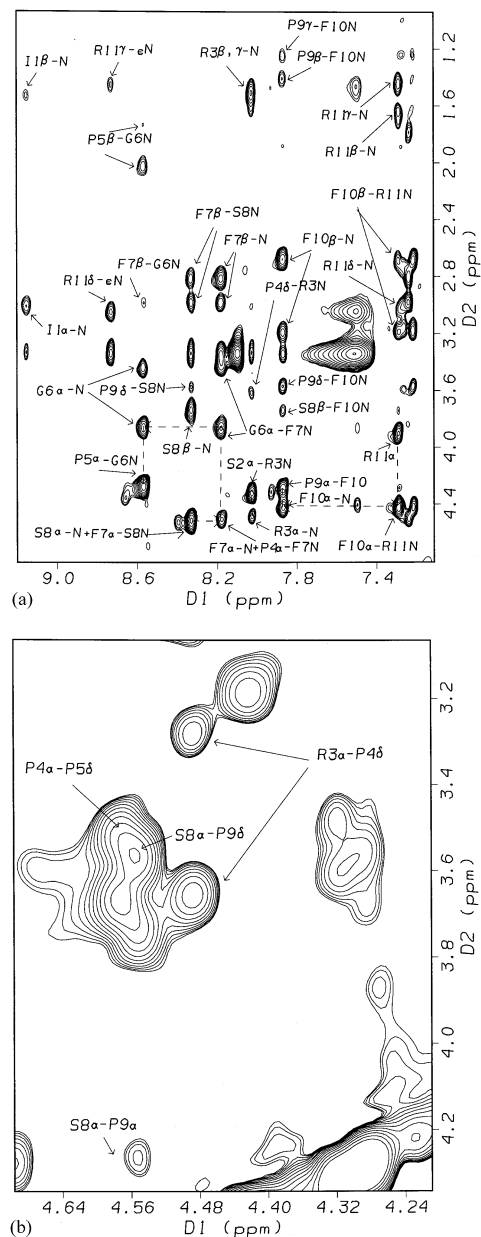


Fig. 2. NOESY spectrum (500 MHz) of T-kinin in DMSO- $d_6$  at 298 K, recorded with mixing time 400 ms. (a) Sequential assignments along with medium range nOe's; (b)  $\alpha$ X- $\delta$ Pro and  $\alpha$ X- $\alpha$ Pro nOe's.

having a *cis* peptide bond. However, strong nOe's between Arg<sup>3</sup>  $\alpha$ H-Pro<sup>4</sup>  $\delta$ H, Pro<sup>4</sup>  $\alpha$ H-Pro<sup>5</sup>  $\delta$ H, and Ser<sup>8</sup>  $\alpha$ H-Pro<sup>9</sup>  $\delta$ H (Fig. 2b) confirm the all *trans* conformation as the major component. The percentage of the *cis* conformation was found to be about 3%, based on intensities of the cross peaks of the minor and major conformations in the TOCSY spectrum.

A weak nOe between Pro<sup>4</sup>  $\alpha$ H-Phe<sup>7</sup> NH and a strong Gly<sup>6</sup> NH-Phe<sup>7</sup> NH interaction suggest a type I  $\beta$ -turn across the segment Pro<sup>4</sup>-Pro<sup>5</sup>-Gly<sup>6</sup>-Phe<sup>7</sup>. A second  $\beta$ -turn at the C-terminal as observed in water is also present here. The strong nOe between Phe<sup>10</sup> NH-Arg<sup>11</sup> NH, supports this observation. The two  $\beta$ -turns are

Table 5

The torsion angles ( $\phi$ ,  $\psi$ ,  $\chi$ ) averaged over the 25 structures obtained in simulation S1 <sup>a,b</sup>

Residue	$\phi$	$\psi$	$\chi_1$	$\chi_2$	$\chi_3$	$\chi_4$	$\chi_5$
Ile <sup>1</sup>	–	–116(0), 175(1)	–56(9)	88(0), 162(4)	–175(0), –56(0), 178(1)	–	–
Ser <sup>2</sup>	–144(3)	–117(0), 177(0)	67(2)	–165(0), –65(4)	–	–	–
Arg <sup>3</sup>	–142(3)	171(1)	–170(11), 178(2)	–163(19), –89(3)	75(7), 172(1)	–154(2), 157(24)	5(4)
Pro <sup>4</sup>	–81(10)	175(2)	–32(3), 20(8)	–34(4), 40(1)	–	–	–
Pro <sup>5</sup>	–68(11)	–115(0), 178(1)	–32(1), 30(3)	–37(1), 40(0)	–	–	–
Gly <sup>6</sup>	–165(13)	–119(0), 180(0)	–	–	–	–	–
Phe <sup>7</sup>	–149(1)	176(1)	–155(1), –75(0)	–99(0), 120(2)	–	–	–
Ser <sup>8</sup>	–152(5)	173(1)	67(2)	–43(3)	–	–	–
Pro <sup>9</sup>	–62(2)	–35(1)	–30(1)	38(0)	–	–	–
Phe <sup>10</sup>	–97(0)	–6(1)	–66(0)	–76(0), 102(0)	–	–	–
Arg <sup>11</sup>	–160(3)	–	–151(2)	51(0), 98(1)	–52(1), 40(0)	–163(1), 173(0)	–14(0), 8(0)

<sup>a</sup> Torsions are in (°).<sup>b</sup> Numbers in parentheses are standard deviation values.

Table 6

The torsion angles ( $\phi$ ,  $\psi$ ,  $\chi$ ) averaged over the 25 structures obtained in simulation S2 <sup>a,b</sup>

Residue	$\phi$	$\psi$	$\chi_1$	$\chi_2$	$\chi_3$	$\chi_4$	$\chi_5$
Ile <sup>1</sup>	–	–39(0), –18(4), 126(8)	58(2)	71(3), 92(0), 161(1)	–65(7)	–	–
Ser <sup>2</sup>	77(2)	–89(1), –68(1)	74(0)	–45(2)	–	–	–
Arg <sup>3</sup>	–90(4)	123(6), 148(7)	–168(2), –70(5)	–171(0), 71(4), 174(2)	174(2)	–158(13), –101(1), 93(6), 169(5)	2(1)
Pro <sup>4</sup>	–71(5)	168(4)	24(2)	–31(1)	–	–	–
Pro <sup>5</sup>	–51(1)	–23(1)	–34(1)	37(0)	–	–	–
Gly <sup>6</sup>	–87(2)	–13(1)	–	–	–	–	–
Phe <sup>7</sup>	58(4)	–72(4)	–151(10), –98(2)	63(3), 87(2)	–	–	–
Ser <sup>8</sup>	–115(5)	152(1)	–175(0)	171(1)	–	–	–
Pro <sup>9</sup>	–57(1)	–23(0)	–14(0)	32(0)	–	–	–
Phe <sup>10</sup>	–93(1)	6(0)	–77(0)	99(0)	–	–	–
Arg <sup>11</sup>	–124(1), –104(3)	–	178(1)	–176(0)	169(3)	–84(2)	2(1), 12(1)

<sup>a</sup> Torsions are in (°).<sup>b</sup> Numbers in parentheses are standard deviation values.

Table 7

The torsion angles ( $\phi$ ,  $\psi$ ,  $\chi$ ) averaged over the 25 structures obtained in simulation S3 <sup>a,b</sup>

Residue	$\phi$	$\psi$	$\chi_1$	$\chi_2$	$\chi_3$	$\chi_4$	$\chi_5$
Ile <sup>1</sup>	–	–83(7)	–30(3)	155(2)	–178(1), –59(1), 64(2)	–	–
Ser <sup>2</sup>	–86(7)	49(1), 78(8)	–172(6), 61(6)	–176(3), 54(3)	–	–	–
Arg <sup>3</sup>	50(4)	171(4)	–82(4)	67(3)	171(1)	–179(0), 168(3)	–3(0)
Pro <sup>4</sup>	–39(1)	–48(2)	–23(3)	2(0)	–	–	–
Pro <sup>5</sup>	–69(1)	–41(1)	22(0)	–36(0)	–	–	–
Gly <sup>6</sup>	–76(1)	–47(1)	–	–	–	–	–
Phe <sup>7</sup>	–59(3)	–43(2)	178(2)	75(3)	–	–	–
Ser <sup>8</sup>	–48(1)	–64(1)	44(3)	–86(3)	–	–	–
Pro <sup>9</sup>	–74(1)	–58(1)	–12(0)	21(1)	–	–	–
Phe <sup>10</sup>	–89(0)	70(1)	–166(2)	–101(4), 79(3)	–	–	–
Arg <sup>11</sup>	–55(2)	–	–145(0)	74(1)	53(1)	78(0)	7(1)

<sup>a</sup> Torsions are in (°).<sup>b</sup> Numbers in parentheses are standard deviation values.

Table 8

Summary of experimental restraints and statistical analysis of family of structures generated by simulated annealing

Parameters	Values in different solvents		
	Water (S1)	DMSO- <i>d</i> <sub>6</sub> (S2)	HFA (S3)
Distance restraints			
All	12	54	103
Intra-residue	4	30	81
Inter-residue	8	24	22
Sequential	8	14	10
Medium range	–	10	12
Long range	–	–	–
Fractional average violation/constraint	0.202 ± 0.02	0.267 ± 0.03	0.075 ± 0.013
Average no. of violations/structure <sup>a</sup>	1.46 ± 0.33	1.68 ± 0.42	1.0 ± 0.0
RMSD's with average structure: backbone atoms			
Maximum	1.892	1.478	0.804
Minimum	0.555	0.416	0.258
Average	1.128 ± 0.421	0.76 ± 0.37	0.39 ± 0.183
Average pair-wise RMSD	1.51 ± 0.82	1.03 ± 0.62	0.51 ± 0.34
IRMA: <i>R</i> -factor	–	0.306	0.399

<sup>a</sup> A ± 0.2 Å difference from the imposed distance restraint was considered a violation.

further supported by low temperature coefficients, for both Phe<sup>7</sup> and Arg<sup>11</sup> amide protons. This is the dominant conformation for the peptide in DMSO-*d*<sub>6</sub>. The existence of other conformations is indicated by the observation of low temperature coefficients for Arg<sup>3</sup> NH and Ser<sup>8</sup> NH, which coexist with the major two β-turn structure. However, unequivocal deduction of the complete structure of the minor conformation is not possible from the limited information presented by the spectra.

Here again, the theoretical methods of secondary structure prediction very unanimously support the β-turn around the tetrad Pro<sup>4</sup>-Pro<sup>5</sup>-Gly<sup>6</sup>-Phe<sup>7</sup>. MD simulations produced a set of structures with the two β-turn motif (Fig. 4b), having an average pair-wise RMSD of only 1.03. This shows that the generated conformers are quite close to each other, as compared to those in water (Table 8) and suggests, a more rigid structure for T-kinin in DMSO-*d*<sub>6</sub>.

Structural aspects of the simulated structures are, a type I β-turn for the two tetrads Pro<sup>4</sup>-Pro<sup>5</sup>-Gly<sup>6</sup>-Phe<sup>7</sup> and Ser<sup>8</sup>-Pro<sup>9</sup>-Phe<sup>10</sup>-Arg<sup>11</sup>; and γ-bends at Ser<sup>2</sup> and Phe<sup>7</sup>. Gly<sup>6</sup> is buried in the first β-turn and has its NH in a hydrogen bond with CO of Pro<sup>4</sup>. This may account for the low temperature coefficient of Gly<sup>6</sup> amide.

Constraint free minimization of the structures obtained by MD simulation, maintained all the secondary structural features. The deviation in the two sets of structures, (with restraints and without restraints), is only 1.1 RMSD for the heavy atoms. This is an excellent test of the stability and validity of the structures, generated using restrained MD.

IRMA refinement of the structures generated by restrained MD simulation gave an average *R*-factor of 0.306.

The two β-turns seen here for T-kinin in DMSO-*d*<sub>6</sub>, has a parallel in earlier studies. We had reported such a structure for BK in DMSO-*d*<sub>6</sub> [19] and for Tyr-Bk [29]. The relationship between conformation and biological activity discussed in the Section 1, and the fact that a two β-turn structure is seen for BK [19], Tyr-Bk [29], T-kinin and the antagonists B-9340 [33] and HOE 140 [34], make it highly probable that, such a state is involved in receptor recognition and activation for BK antagonists and agonists. Support for this postulation comes from the BK antagonist MEN 11270, that has been constrained by cyclization at the C-terminal to adopt a β-turn, and has a p*K*<sub>i</sub> of 10.3 nM [35]. Further, a turn like structure at the N-terminal end in the highly potent antagonists (D-Arg<sup>0</sup>, Hyp<sup>3</sup>, Thi<sup>5</sup>, D-Cpg<sup>7</sup>, Cpg<sup>8</sup>)-BK and (D-Arg<sup>0</sup>, Hyp<sup>3</sup>, D-Cpg<sup>7</sup>, Cpg<sup>8</sup>)-BK [36], adds weight to the suggestion of a two β-turn structure in BK and its variants, as a requirement for biological activity.

### 2.3. Conformation in HFA

The TOCSY spectrum shows only one set of peaks. NOe's are observed between Arg<sup>3</sup> αH-Pro<sup>4</sup> δH, Pro<sup>4</sup> αH-Pro<sup>5</sup> δH and Ser<sup>8</sup> αH-Pro<sup>9</sup> δH, which identify a conformation with prolines in an all *trans* fashion.

A number of both short and long range inter-residue nOe's are observed, these being *i* – *i* + 1 (αH-NH, NH-NH, αH-αH, βH-NH), medium range peaks like *i* – *i* + 2 (NH-NH), *i* – *i* + 3 (αH-NH, αH-βH) and long range

$i - i + 4$  ( $\alpha$ H-NH) peaks. The pattern of both sequential and medium range nOe's (Fig. 3), suggest the presence of a helical structure for the peptide in HFA. The low temperature coefficients for almost all the amide protons, further support this structure. It should be noted here that, the criteria for predicting intramolecular H-bonding from temperature coefficients of NH chemical shifts in HFA, is different from water. In water, temperature coefficients below  $3.00 \text{ ppb K}^{-1}$ , are suggestive of intramolecular H-bonds [37], while in solvents like TFE/HFA this limit is suggested to be more than  $5.0 \text{ ppb K}^{-1}$  [38].

The  $\alpha^{13}\text{C}$  chemical shift index (CSI) for almost all residues between Arg<sup>3</sup> and Arg<sup>11</sup> are in line with a helical structure for the peptide in HFA [39,40].

MD simulations produced an *ensemble* of structures with average pair-wise RMSD of 0.51. The average phi and psi values of the resultant structures (Table 7) show a  $\alpha$ -helix like structure spanning residues Arg<sup>3</sup> to Arg<sup>11</sup> (Fig. 4c). The quality of the simulated structures can be

judged by a negligible violation on the imposed distance restraints. Constraint free minimization of these structures, maintained the overall  $\alpha$ -helix like structure, indicating that it is indeed a stable structure. The average RMSD between the two sets of structures was found to be 0.35. The average IRMA *R*-factor for the simulated structures is 0.39.

None of the earlier studies on BK, or its agonists or antagonists, have reported a helical structure. The observation that T-kinin adopts a  $\alpha$ -helix like structure in HFA is likely a result of the influence of the solvent. More evidence is needed to define exactly what role, if any, the  $\alpha$ -helix plays in receptor recognition by BK and its analogs.

### 3. Conclusion

NMR and molecular modeling studies of T-kinin show that, the peptide can adopt different

	I1	S2	R3	P4	P5	G6	F7	S8	P9	F10	R11
$d_{\alpha, N(i,i+1)}$	—————										

(a)

	I1	S2	R3	P4	P5	G6	F7	S8	P9	F10	R11
$d_{\alpha, N(i,i+1)}$		—————			—————				—————		
$d_{N, N(i,i+1)}$						—————				—————	
$d_{\beta, N(i,i+1)}$					—————		—————		—————		
$d_{\alpha, N(i,i+3)}$				—————							

(b)

	I1	S2	R3	P4	P5	G6	F7	S8	P9	F10	R11
$d_{\alpha, N(i,i+1)}$	—————				—————				—————		
$d_{N, N(i,i+1)}$		—————				—————				—————	
$d_{\alpha, \alpha(i,i+1)}$			—————		—————						
$d_{\beta, N(i,i+1)}$	—————				—————		—————		—————		
$d_{N, N(i,i+2)}$								—————		—————	
$d_{\alpha, N(i,i+3)}$				—————	—————		—————		—————		
$d_{\alpha, \beta(i,i+3)}$		—————		—————			—————	—————			
$d_{\alpha, N(i,i+4)}$			—————	—————	—————		—————	—————			

(c)

Fig. 3. Survey of backbone nOe's observed for T-kinin in: (a) water; (b) DMSO- $d_6$ ; and (c) HFA.



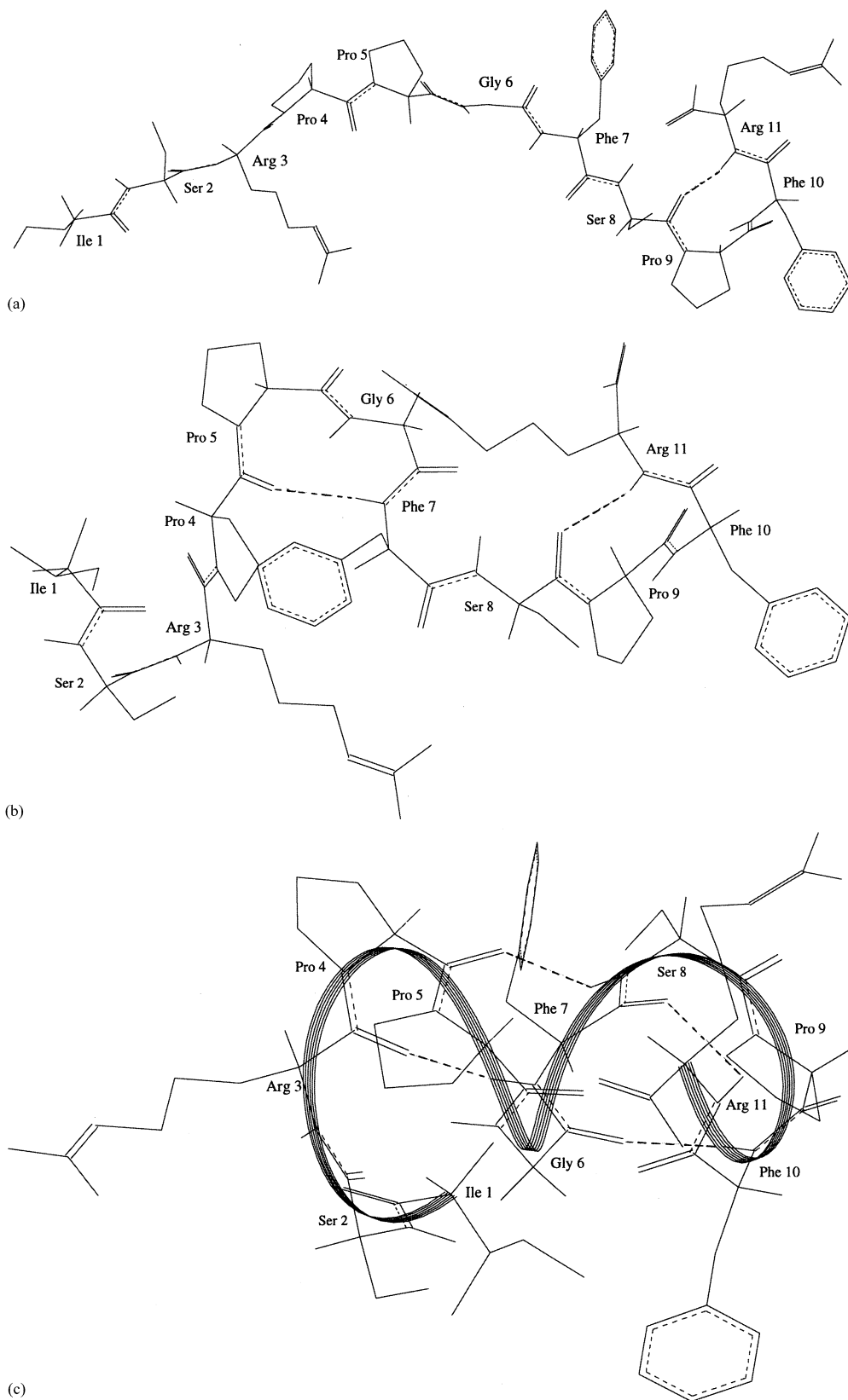


Fig. 4. Structure of T-kinin in: (a) water; (b) DMSO- $d_6$ ; and (c) HFA as obtained by MD simulations.

conformations depending on the solvent. Structures with  $\beta$ -turn are seen in both DMSO- $d_6$  and water, while HFA promotes a  $\alpha$ -helix like structure. The equal activity of T-kinin with BK can then be explained by the fact that both are capable of acquiring a  $\beta$ -turn at the C-terminal which is the key requirement for B2 receptor interaction as also expressed by potent antagonists like HOE 140 [34] and MEN 11270 [35]. We note that, though BK has been found to possess no stable structure in water, studies in other environments that can be closely linked to receptor states [22], have identified a  $\beta$ -turn at the C-terminal end as being the preferred binding conformation for BK.

ACE present in human plasma (a medium closer to water) hydrolyses BK more readily than T-kinin. This stems from the fact that in water BK has an extended or random coil like structure that is more 'open' to cleavage by ACE. T-kinin has been shown to possess a  $\beta$ -turn at the C-terminal end in water and thus may interact very weakly with ACE, resisting hydrolysis. Underlining this argument is the probability that structure stabilization in plasma is less likely compared to a receptor environment and therefore the structures of both molecules in water can be extrapolated to their ACE binding potential.

## 4. Experimental

### 4.1. Sample preparation

The peptide T-kinin (as acetate salt) and DMSO- $d_6$  (99.9%) were purchased from Sigma Chemical Co. (USA), D<sub>2</sub>O and DSS from Merck (Germany), and HFA from Aldrich Chemical Co. (USA).

T-kinin (2 mg) was dissolved in 0.5 mL DMSO- $d_6$  (3 mM solution) in a nitrogen atmosphere. For studies in water, the same amount of peptide was dissolved in a 0.6 mL solution of 95% H<sub>2</sub>O–5% D<sub>2</sub>O mixture to give a 2.5 mM solution. To study the effect of HFA, a mixture of 55% H<sub>2</sub>O–40% HFA–5%D<sub>2</sub>O was used. About 10  $\mu$ L of a 0.1% solution of DSS in appropriate solvent was used as internal standard for the three solvents. The pH of aq. samples was adjusted to 4.0 using dilute NaOH. The solutions were filtered and transferred to 5 mm NMR tubes.

### 4.2. NMR

All NMR experiments for DMSO- $d_6$ , except the HSQC spectrum, were carried out on a Bruker AMX 500 MHz FT-NMR spectrometer using a 5 mm inverse detection (ID) probe with 90° proton pulse length of 9  $\mu$ s at 2 db attenuation. Data were collected with XWINNMR (v. 1.3) on a Silicon Graphics O2 workstation. All experiments for water and HFA, and HSQC

for DMSO- $d_6$  were performed on a Varian Unity Plus 600 MHz FT-NMR spectrometer using a 5 mm ID probe with 90° proton pulse length of 7.5  $\mu$ s at a transmission power of 60 db. Data were collected using V-NMR (v. 6.1 b) on a Sun Sparc workstation. In both cases, the length of the 90° pulse was checked at the beginning of the session and the temperature was controlled throughout the experiments to  $\pm 0.1$  K. The data were processed using FELIX software (v. 97, MSI, USA) running on a Silicon Graphics O2 workstation. All 2D spectra were acquired without spinning, whereas samples were spun (at 20 rpm) for all 1D experiments. 1D-NMR spectra of serially diluted samples were recorded to confirm that the peptide does not aggregate under the conditions of study.

All experiments on Bruker AMX 500 MHz were recorded with time proportional phase increment (TPPI) [41] for quadrature detection in the D1 dimension, whereas the States-Haberkorn [42] method of quadrature detection was followed on the Varian Unity Plus 600 MHz instrument. A sweep width of 7000 Hz for spectra recorded on Bruker and 8000 Hz for those on Varian machine was used in both dimensions. Typically, 2 K data points in D2 and 512 experiments in D1 were acquired. All 2D experiments were preceded with 32 dummy scans, but none were applied between individual D1 increments. The pre-acquisition  $\alpha$  was individually adjusted. A relaxation delay of 1.5 s was used for all experiments.

The TOCSY experiment [43,44] was carried out with the basic pulse sequence proposed by Bax. A 2 ms trim pulse preceded the MLEV-17 spin lock of 80 ms. ROESY [45] with a mixing time of 300 ms was also recorded. The mixing was achieved by continuous wave. Standard pulse sequences for DQF-COSY [46] and NOESY [47] were used. Several NOESY spectra with mixing times of 50, 100, 150, 250 and 400 ms were recorded. <sup>1</sup>H-<sup>13</sup>C Gradient-HSQC experiments [48] with sensitivity enhancement was recorded to obtain <sup>13</sup>C chemical shifts.

For the samples in water and HFA, solvent suppression was achieved using the WATERGATE (Water suppression by Gradient Tailored Excitation) technique for TOCSY [49] and NOESY [50] experiments. The number of transients per t1 increment for DQF-COSY was 64, 96 for HSQC and 32 for all other experiments.

A  $\pi/2$  phase-shifted sine squared window function was applied to the data along both dimensions. In some spectra,  $\pi/4$  phase-shifted sine squared window function was used to obtain better resolution when the peaks overlapped. The data was zero filled to a matrix of size 2 K  $\times$  2 K points prior to Fourier transformation. Chemical shifts were referenced to DSS.

Temperature coefficients for amide protons were determined from two TOCSY experiments carried out at 298 and 308 K for DMSO- $d_6$  and at 283 and 298 K for

water and HFA. All other experiments for DMSO- $d_6$  and water samples were recorded at 298 K and for HFA at 283 K  $^3J_{\text{NH}\alpha}$  coupling constants were extracted from the 1D spectra.

Identification of spin systems was done using DQF-COSY and TOCSY and sequential assignments were made according to the methods described by Wüthrich [51].

### 4.3. Theoretical methods

#### 4.3.1. Secondary structure prediction

Methods available in the BIOPOLYMER module in SYBYL (v. 6.4 Tripos, USA) were employed. We have used the methods developed by Qian/Sejnowski (based on Neural Networks) [52], Garnier–Osguthorpe–Robson (employing Information Theory) [53] and Maxfield/Scheraga (using Bayes Statistics) [54], for predicting the most likely secondary structure for the peptide.

#### 4.3.2. Chemical shift index (CSI)

The CSI of a proton is defined as the difference between the measured chemical shift and the chemical shift for that proton when the peptide is in a random coil structure. A negative deviation of  $\alpha\text{H}$  chemical shift from the random coil value for a stretch of at least three or four residues, suggests that, helical or turn-like structures prevail, while a positive deviation, indicates the presence of a  $\beta$ -sheet structure [55]. For  $\alpha^{13}\text{C}$ , the relationship between the deviation (positive or negative) from the random coil values, and the secondary structure, is opposite to that described above for the proton.

### 4.4. Structure calculation

#### 4.4.1. Molecular dynamics (MD) simulations

The secondary structure of a molecule can be deduced from the NMR parameters of chemical shift, temperature coefficients and nOe's, coupled with various molecular modeling tools. We have used MD simulations with distance and dihedral restraints, to generate the solution structures of our peptide. In addition, a 'free' MD simulation, without restraints, was also carried out to determine the various structural patterns the peptide could possibly adopt. Computations were done on a Silicon Graphics O2 workstation, with molecular modeling software from MSI, USA (INSIGHT II and DISCOVER, version 98). An extended structure of the peptide was built with the BIOPOLYMER module as the starting conformation for the simulations. The energy of the system was calculated by the consistent valence forcefield (CVFF) [56]. During the simulations, the *omega* torsions were forced to  $180^\circ$  with a force constant of  $100 \text{ kcal mol}^{-1} \text{ rad}^{-2}$ . The bond stretching in the energy equation was represented by a harmonic function. A dielectric constant of 1.0

was used for evaluation of the electrostatics. The Newton's equations of motion were integrated with the Verlet algorithm [57], with a step size of 1 fs. During equilibration, temperature was controlled by direct scaling of the atom velocities, while during the data collection period, a weak coupling to a temperature bath with a time constant of 0.1 ps was used. Distance and dihedral restraints were applied for all restrained simulations as discussed further. Three restrained simulations (S1, S2, S3), each utilizing NMR data obtained for the peptide in water, DMSO- $d_6$  and HFA, respectively, were performed with the general methodology as stated below. In all three simulations, the starting extended structure was thoroughly minimized by a combination of steepest descents and conjugate gradients, to a gradient of  $0.01 \text{ kcal mol}^{-1} \text{ \AA}^{-1}$ . In simulations S1 and S2 this was followed by an MD run at 300 K, beginning with 3 ps of equilibration, and 25 ps of productive dynamics. In case of simulation S3, the dynamics was conducted at 600 K. The temperature was reached by a slow 'heating' in 100 K steps with a 2.5 ps dynamics run. As in the previous simulations, the data collection period was restricted to 25 ps. These 25 structures were then 'cooled' to 300 K, in steps of 100 K, by a 2.5 ps dynamics. The 300 K structures, in all three simulations, (each 25 in number), were then energy minimized by steepest descents, followed by conjugate gradients, and ending with the Newton–Raphson (VA09A) method, to yield structures having a gradient of  $0.001 \text{ kcal mol}^{-1} \text{ \AA}^{-1}$  or lower. The stability of the solution conformations was proved by final minimization without NMR restraints. For 'free' simulation, the structure, obtained by thorough minimization of the starting extended structure, was 'heated' to 1000 K in steps of 100 K with a 2.5 ps dynamics run followed by 100 ps of productive dynamics. These 100 structures were processed in a similar manner as for simulation S3.

#### 4.4.2. Restraints

**4.4.2.1. Distance restraints.** Approximate distance restraints were calculated from the linear portion of the nOe build up curve, using the relationship  $\eta_{ij}/\eta_{kl} = (r_{kl}/r_{ij})^6$ , where  $\eta_{ij}$  and  $\eta_{kl}$  are the nOe intensities for the atom pairs  $i, j$  and  $k, l$  separated by distances  $r_{ij}$  and  $r_{kl}$ , respectively. The intensity of the nOe between  $\beta$  protons of Pro<sup>9</sup> for DMSO- $d_6$ , and  $\delta$  protons of Pro<sup>4</sup> for water and HFA, whose distance is  $1.74 \text{ \AA}$ , was used as the reference. The distances calculated for methyl and methylene groups, were corrected according to the rules formulated by Wüthrich [51]. The distances were cast as restraints, using force constants that ranged from 1 to  $35 \text{ kcal mol}^{-1} \text{ rad}^{-2}$  and a  $\pm 0.3 \text{ \AA}$  range put on the calculated distances, to represent the upper and lower bounds. The total number of distance restraints in the

second and third simulations, was 54 and 103, respectively. Only few accurate distances could be extracted from the water spectrum, limiting the number of distance restraints to 10.

**4.4.2.2. Dihedral restraints.** The  $^3J_{\text{NH}\alpha}$  coupling is a function of the dihedral angle  $\phi$ , as given by the modified Karplus equation [58]

$$^3J_{\text{NH}\alpha} = 6.51 \cos^2(\phi - 60) - 1.76 \cos(\phi - 60) + 1.60$$

The coupling constants were transformed to  $\phi$  values, and introduced as dihedral restraints, allowing a range of  $\pm 10^\circ$  on the calculated values. Force constants in the range of 1–30 kcal mol<sup>-1</sup> rad<sup>-2</sup>, were applied. As many coupling constants that could be accurately estimated, were used as restraints.

#### 4.4.3. Iterative relaxation matrix analysis (IRMA)

IRMA is a computational method based on NMR relaxation theory [59]. For a given molecular structure, the nOe intensities can be accurately calculated by IRMA, since it takes into consideration, the entire spin-relaxation network and molecular flexibility. The calculated and experimental nOe's are compared, and the structure is changed gradually, until the two match as close as possible.

We have used IRMA on each set of 25 structures generated by the two simulations S2 and S3, to evaluate the precision and accuracy of these NMR structures. This is measured by the *R*-factor defined as follows [60]

$$R = \frac{\sum_{ijm} W_{ij}(\tau_m) |A_{ij}^{\text{calc}}(\tau_m) - A_{ij}^{\text{exp}}(\tau_m)|}{\sum_{ijm} W_{ij}(\tau_m) A_{ij}^{\text{exp}}(\tau_m)}$$

where  $A_{ij}^{\text{calc}}(\tau_m)$  and  $A_{ij}^{\text{exp}}(\tau_m)$  denotes, respectively, the theoretical and experimental nOe intensities, for the pair  $(i, j)$ , for a given mixing time ( $\tau_m$ ). Weight factors  $W_{ij}(\tau_m)$ , which account for measurement errors, particularly noise levels, were set to 1.0.

The rotational correlation time ( $\tau_c$ ) for the molecule, was estimated as 3 ns for DMSO-*d*<sub>6</sub>, and 2 ns for water and HFA, from the nOe buildup of the reference peak, for respective samples [61].

For small peptides *R*-factor in the range of 0.30–0.50 has been reported [60,62]. This is considered a reasonably good value in view of the sparse NMR data generally observed for these molecules [61].

#### Acknowledgements

The All India Council of Technical Education (AICTE) and the Ministry of Human Resource and Development (MHRD) are thanked for the computational facilities at Bombay College of Pharmacy. The

facilities provided by the National Facility for High Field NMR located at TIFR are gratefully acknowledged. P.D. thanks Council of Scientific and Industrial Research for a research fellowship. We thank Dr K.I. for his valuable comments on the manuscript.

#### References

- [1] D.J. Campbell, *Braz. J. Med. Biol. Res.* 33 (2000) 665–677.
- [2] T.L. Goodfriend, D.L. Ball, *J. Lab. Clin. Med.* 73 (1969) 501–511.
- [3] D. Ragoli, J. Barabe, *Pharmacol. Rev.* 32 (1980) 1–46.
- [4] S.G. Farmer, R.M. Burch, in: R.M. Burch (Ed.), *Bradykinin Antagonists, Basic and Clinical Research*, Marcel Dekker, New York, 1991, pp. 1–31.
- [5] A. Kuoppala, K.M. Lindstedt, J. Saarinen, P.T. Kovanen, J.O. Kokkonen, *Am. J. Physiol. Heart Circ. Physiol.* 278 (2000) H1069–H1074.
- [6] H. Okamoto, L.M. Greenbaum, *Biochem. Biophys. Res. Commun.* 112 (1983) 701–708.
- [7] P. Lopes, R. Couture, *Eur. J. Pharmacol.* 210 (1992) 137–147.
- [8] X. Gao, J.M. Stewart, R.J. Vavrek, L.M. Greenbaum, *Biochem. Pharmacol.* 46 (1993) 1607–1612.
- [9] I. Yamawaki, J. Tamaoki, Y. Takeda, A. Chiyotani, N. Sakai, S. Kameyama, K. Konno, *J. Appl. Physiol.* 79 (1995) 1129–1133.
- [10] Y. Takeda, J. Tamaoki, I. Yamawaki, A. Chiyotani, K. Konno, *Nihon. Kyobu. Shikkan. Gakkai. Zasshi.* 34 (1996) 627–631.
- [11] J.A. Santiago, H.C. Champion, P.J. Kadowitz, *Am. J. Physiol.* 272 (1997) H1491–H1498.
- [12] H.C. Champion, J.A. Santiago, M.A. Czaplá, T.J. Bivalacqua, C. Ilgenfritz, P.J. Kadowitz, *Peptides* 18 (1997) 1357–1364.
- [13] A. Barlas, K. Sugio, L.M. Greenbaum, *FEBS. Lett.* 190 (1985) 268–270.
- [14] G. Wunderer, I. Walter, E. Muller, A. Henschen, *Biol. Chem. Hoppe. Seyler.* 367 (1986) 1231–1234.
- [15] G. Wunderer, I. Walter, B. Eschenbacher, M. Lang, J. Kellermann, G. Kindermann, *Biol. Chem. Hoppe. Seyler.* 371 (1990) 977–981.
- [16] N.E. Rhaleb, G. Drapeau, S. Dion, D. Jukic, N. Rouissi, D. Regoli, *Br. J. Pharmacol.* 99 (1990) 445–448.
- [17] K.T. Passaglio, M.A. Vieira, *Immunopharmacology* 32 (1996) 166–168.
- [18] L. Denys, A.A. Bothner-By, G.H. Fisher, J.W. Ryan, *Biochemistry* 21 (1982) 6531–6536.
- [19] S.R. Mirmira, S. Durani, S. Srivastava, R.S. Phadke, *Magn. Reson. Chem.* 28 (1990) 587–593.
- [20] S. Srivastava, R.S. Phadke, G. Govil, in: V. Renugopalkishnan, P.R. Carey, I.C.P. Smith, S.G. Huang, A.C. Storer (Eds.), *Proteins: Structure, Dynamics and Design*, Escom, Leiden, The Netherlands, 1991, pp. 57–61.
- [21] J.R. Cann, X. Liu, J.M. Stewart, L. Gera, G.A. Kotovych, *Biopolymers* 34 (1994) 869–878.
- [22] S.C. Lee, A.F. Russel, W.D. Laidig, *Int. J. Pept. Protein Res.* 35 (1990) 367–377.
- [23] E.G. Erdoc, in: E.G. Erdoc (Ed.), *Handbook of Experimental Pharmacology*, Springer-Verlag, New York, 1970, p. 25.
- [24] E.D. Nicolaides, H.A. Dewald, M.K. Craft, *J. Med. Chem.* 6 (1963) 739–741.
- [25] S. Srivastava, S.S. Rai, R.S. Phadke, *Phys. Med.* 8 (1992) 137–141.
- [26] M.L. Mashford, M.L. Roberts, *Biochem. Pharmacol.* 20 (1971) 969–973.
- [27] S. Srivastava, S. Haram, R.S. Phadke, *Magn. Reson. Chem.* 29 (1991) 333–337.

- [28] C.E. Ody, T.L. Goodfriend, C. Pena, *Biochem. Pharmacol.* 29 (1980) 175–185.
- [29] S. Srivastava, R.S. Phadke, S.A. Kamath, E.C. Coutinho, *Eur. J. Med. Chem.* 32 (1997) 669–675.
- [30] B. Matthias, *Quat. Rev. Biophys.* 31 (1998) 297–355.
- [31] R. Rajan, S.K. Awasthi, S. Bhattacharjya, P. Balram, *Biopolymers* 42 (1997) 125–128.
- [32] R.E. London, J.M. Stewart, J.R. Cann, N.A. Matwiyoff, *Biochemistry* 17 (1978) 2270–2283.
- [33] J. Sejbal, J.R. Cann, J.M. Stewart, L. Gera, G. Kotorych, *J. Med. Chem.* 39 (1996) 1281–1292.
- [34] W. Guba, R. Haessner, G. Breipohl, S. Henke, J. Knolla, V. Santagada, H. Kessler, *J. Am. Chem. Soc.* 116 (1994) 7532–7540.
- [35] S. Meini, L. Quartara, A. Rizzi, R. Patacchini, P. Cucchi, A. Giolitti, G. Calo, D. Regoli, M. Criscuoli, C.A. Maggi, *J. Pharmacol. Exp. Ther.* 289 (1999) 1250–1256.
- [36] X. Liu, J.M. Stewart, L. Gera, G. Kotovych, *Biopolymers* 33 (1993) 1237–1247.
- [37] A.C. Bach II, C.Y. Eyermann, J.D. Gross, M.J. Bower, R.L. Harlow, P.C. Weber, W.F. Degrado, *J. Am. Chem. Soc.* 116 (1994) 3207–3209.
- [38] P. Khandelwal, S. Seth, R.V. Hosur, *Eur. J. Biochem.* 264 (1999) 468–478.
- [39] M.A. Jimenez, J.L. Nieto, J. Herranz, M. Rico, J. Santoro, *FEBS. Lett.* 221 (1987) 320–324.
- [40] G. Merutka, J.H. Dyson, P.E. Wright, *J. Biomol. NMR* 5 (1995) 14–24.
- [41] D. Marion, K. Wüthrich, *Biochem. Biophys. Res. Commun.* 113 (1983) 967–974.
- [42] D.J. States, R.A. Haberkorn, D.J. Ruben, *J. Magn. Reson.* 48 (1982) 286–292.
- [43] L. Braunschweiler, R.R. Ernst, *J. Magn. Reson.* 53 (1983) 521–528.
- [44] A.D. Bax, D.G. Davis, *J. Magn. Reson.* 65 (1985) 355–360.
- [45] A.A. Bothner-By, R.L. Stephens, J. Lee, C.D. Waren, R.W. Jeanloz, *J. Am. Chem. Soc.* 106 (1984) 811–813.
- [46] U. Piantini, O.W. Sorenson, R.R. Ernst, *J. Am. Chem. Soc.* 104 (1982) 6800–6801.
- [47] S. Macura, Y. Huang, D. Suter, R.R. Ernst, *J. Magn. Reson.* 43 (1981) 259–281.
- [48] L.E. Kay, P. Keifer, T. Sarrinen, *J. Am. Chem. Soc.* 114 (1992) 10663–10665.
- [49] C. Dhallium, J.M. Wieruszski, G. Lippens, *J. Magn. Reson. Ser. B.* 111 (1996) 168–170.
- [50] G. Lippens, C. Dhallium, J.M. Wieruszski, *J. Biomol. NMR.* 5 (1995) 327–333.
- [51] K. Wüthrich (Ed.), *NMR of Proteins and Nucleic Acids*, Wiley, New York, 1986.
- [52] N. Qian, T. Sejnowski, *J. Mol. Biol.* 202 (1988) 865–884.
- [53] J. Garnier, D. Osguthorpe, B. Robson, *J. Mol. Biol.* 120 (1978) 97–120.
- [54] F.R. Maxfield, H.A. Scheraga, *Biochemistry* 15 (1976) 5138–5153.
- [55] D.S. Wishart, B.D. Sykes, in: T.L. James, N.J. Oppenheimer (Eds.), *Methods in Enzymology*, vol. 239, Academic Press, San Diego, 1994, pp. 363–392.
- [56] J. Maple, U. Dinur, A.T. Hagler, *Proc. Natl. Acad. Sci. USA* 85 (1988) 5350–5354.
- [57] L. Verlet, *Phys. Rev.* 159 (1967) 98–103.
- [58] G.W. Vuister, A. Bax, *J. Am. Chem. Soc.* 115 (1993) 7772–7777.
- [59] R. Boelens, T.M.G. Koning, R. Kaptein, *J. Mol. Str.* 173 (1988) 299–311.
- [60] C. Gonzales, J.A.C. Rullmann, A.M.J.J. Bonvin, R. Boelens, R. Kaptein, *J. Magn. Reson.* 91 (1991) 659–664.
- [61] *NMRchitect User Guide*, version 2.3, Biosym Technologies, San Diego, 1993.
- [62] A.B. Patel, S. Srivastava, E. Coutinho, R.S. Phadke, *Biopolymers* 50 (1999) 602–612.